



Review—Influence of Corrosion Reactions on the Pulse Electrodeposition of Metals and Alloys

T. A. Green^z  and S. Roy^{*}

Department of Chemical and Process Engineering, University of Strathclyde, Glasgow, Scotland G1 1XJ, United Kingdom

In the electrodeposition of metal and alloys by pulse plating, the importance of the pulse off-time is often neglected. Traditionally it is considered an electrochemically inactive period, allowing, for example, the relaxation of concentration gradients, desorption of additives, recrystallisation and discharge of the double layer capacitance. However, more recent studies have shown that it is possible to have corrosion processes occurring in the off-time which can significantly influence the deposit properties and current efficiency. This has been observed in both aqueous and non-aqueous systems, and appears a very general phenomenon. Typically, in these systems, corrosion is caused by dissolved oxygen or via comproportionation reactions. Similarly, during the pulse electrodeposition of binary and ternary alloys from aqueous and non-aqueous solutions, displacement (corrosion) reactions have been observed in the off-time that can alter the alloy composition and microstructure. The main aim of this paper is to review these various types of corrosion, establish the conditions under which they occur, and quantify their effects related to deposit characteristics, current efficiency and alloy composition.

© 2023 The Author(s). Published on behalf of The Electrochemical Society by IOP Publishing Limited. Content from this work may be used under the terms of the [Creative Commons Attribution 4.0 license](https://creativecommons.org/licenses/by/4.0/). Any further distribution of this work must maintain attribution to the author(s) and the title of the work, journal citation and DOI. [DOI: [10.1149/1945-7111/ad11b4](https://doi.org/10.1149/1945-7111/ad11b4)]



Manuscript submitted November 2, 2023; revised manuscript received November 22, 2023. Published December 11, 2023. *This paper is part of the JES Focus Issue on Pulse Electrolysis, Industrial Electrochemical Engineering, and Scale-Up: In Honor of E. Jennings (EJ) Taylor.*

Pulse plating is a versatile surface finishing technique which has been employed to deposit a wide range of materials including metals, alloys, multilayers, composite coatings and semiconductors.^{1–5} By judicious choice of pulse parameters it is possible to influence the mass transport, kinetics and electro-crystallisation aspects of the deposition process and obtain materials with modified or enhanced characteristics relative to those obtained in conventional DC plating. A monograph¹ edited by Puipe and Leaman and published in 1986 outlined the important theoretical and experimental aspect of pulse plating, and in 2012 this was updated by a monograph² authored by Hansal and Roy. Additionally, a number of useful review articles on the subject of pulse plating have also been published in recent years.^{3–5}

Most theoretical and experimental studies of pulse plating relate to enhancements in mass transport characteristics,^{6–12} kinetics,^{1,2} electrocrystallisation^{13,14} and the importance of double layer charging and discharging effects.^{1,4,15} These effects can only be realised by the correct choice of pulse parameters, and some practical guides and tutorials outlining their rational choice have been published.^{5,16,17} In the case of pulse plating with rectangular unipolar current pulses (Fig. 1, we can define an on-time of duration, t_{on} , and a peak cathodic current density, $i = i_p$, followed by an off-time of duration, t_{off} , where $i = 0$. The pulse period, T , is given by $T = t_{on} + t_{off}$ and the duty cycle, θ , is defined as: $\theta = t_{on}/T = t_{on}/(t_{on} + t_{off})$. Effectively in pulse plating, there are three pulse parameters (i.e. i_p , t_{on} and t_{off}) that need to be selected and optimised.

As deposition occurs in the on-time, the selection of i_p and t_{on} are particularly critical, but the choice of the off-time (or equivalently the duty cycle) is also important. For example, it must be chosen to be sufficiently long to allow concentration gradients formed in the on-time to fully relax and the double layer capacitance to be discharged.^{1,2,4,17} However, beyond these constraints, the off-time is generally considered a relatively unimportant period in pulse plating, limited to some secondary effects related to the adsorption/desorption of additives, impurities and reaction intermediates, and recrystallisation. Figure 1 summarises some of the important effects that may occur during the on and off-times in pulse plating.

However, some early^{6,18} and more recent^{19–21} studies have shown that it is possible to have corrosion processes occurring during the off-time which can significantly influence deposit properties and current efficiency. This has been observed for the pulse plating of certain

metals (e.g. Au and Cu) and can arise due to conventional oxygen-induced corrosion,^{6,19} or alternatively, by comproportionation reactions.^{18–21} Similarly, during the pulse electro-deposition of binary and ternary alloys from aqueous and non-aqueous solutions, displacement (corrosion) reactions have been observed in the off-time that can significantly alter the alloy composition and microstructure.^{22–24} This effect has been more extensively studied, and has been reported in both aqueous^{22–40} and non-aqueous^{41–43} systems. It has also been observed^{44,45} in the pulse electrodeposition of metal multilayers, where it represents an additional complication in estimating layer thickness and composition.

The main objective of the present review is to investigate the overall importance of corrosion effects in the pulse electrodeposition of metals and alloys. A primary aim is to review systems where such corrosion effects have been reported with an aim to understanding the underlying corrosion mechanism, and rationalising the types of corrosion behaviours reported. In particular, we wish to establish the conditions under which they occur, and quantify their effects related to deposit characteristics, current efficiency and alloy composition. Given that corrosion in pulse plating is generally considered undesirable (e.g. lowering current efficiency, and modifying alloy composition or layer thickness) another key objective is to identify conditions where such corrosion effects can be minimised or eliminated entirely. A secondary aim is to evaluate these effects in the electrodeposition-redox replacement (EDRR) process which implements a variant of pulse plating to recover metals ions from waste streams. In the EDRR process, displacement and conventional corrosion reactions can both occur during the off-time.

Simplified Corrosion Analysis

Corrosion during the off-time in pulse plating can manifest itself in a number of forms. The most probable is conventional corrosion due to oxidants such as O_2 or H^+ and the likelihood of this for any metal can be initially assessed using a Pourbaix diagram. Another corrosion type commonly encountered in these systems is comproportionation where the oxidant is a metal ion of higher oxidation state. In the case of metal deposition, the main influence of these corrosion reactions is to reduce the deposition rate and current efficiency, ϵ . These effects can be seen more explicitly if it is assumed that the corrosion rate in the off-time occurs at a constant rate of i_{corr} . This is likely to be the case when the oxidant is reacting at the surface under mass-transport control. Under these conditions, the overall current efficiency, ϵ , can be related to the pulse

^{*}Electrochemical Society Member.

^zE-mail: todd.green@strath.ac.uk

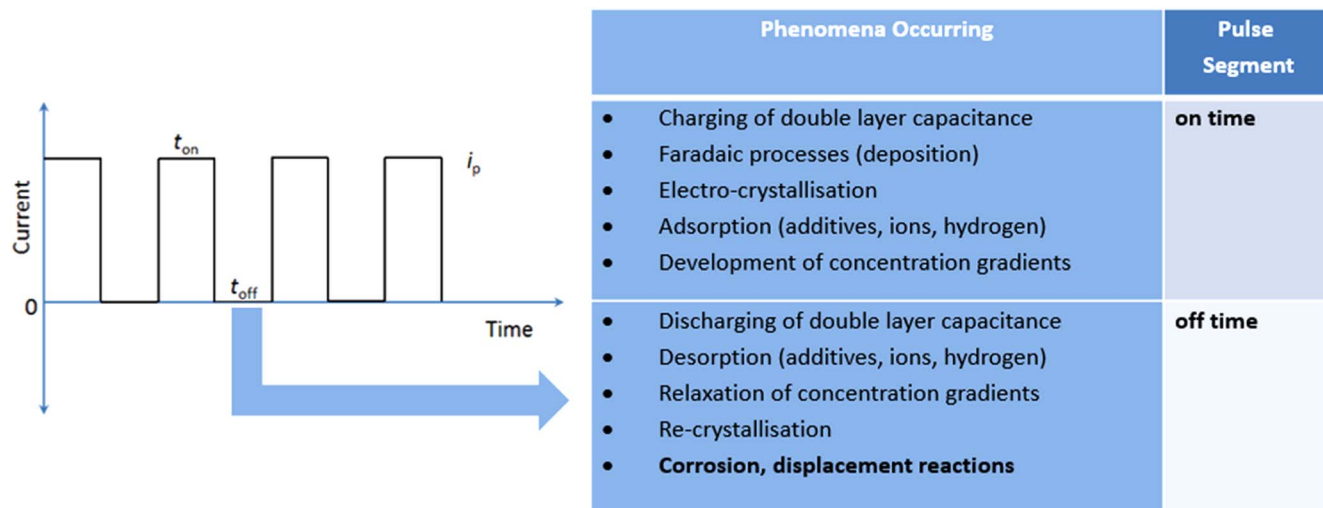


Figure 1. Summary of important pulse parameters and various processes that can occur during the on and off-times.

parameters as follows:

$$\varepsilon = \varepsilon' - i_{\text{corr}} t_{\text{off}} / i_p t_{\text{on}} \quad [1]$$

where ε' is the current efficiency in the absence of any corrosion. Noting that $\theta = t_{\text{on}} / (t_{\text{on}} + t_{\text{off}})$ this expression can be rewritten more conveniently in terms of the duty cycle:

$$\varepsilon = \varepsilon' - i_{\text{corr}} (1 - \theta) / i_p \theta \quad [2]$$

In deriving these expressions, it is assumed that the number of electrons involved in the deposition and dissolution steps are the same. This is normally the case but there are some exceptions, and in previous papers^{20,21} a variant of Eq. 2 was used to reflect this. Figure 2 plots this equation to show the dependence of the overall current efficiency, ε , on the dimensionless parameters θ and i_{corr}/i_p , and illustrates the conditions under which the influence of corrosion is significant.

Another possible corrosion process associated with the pulse plating of alloys involves displacement reactions, where the oxidant

is a more noble metal ion which deposits on the surface and induces dissolution of the less noble metal. The main effect of the displacement reaction is to modify the composition of the alloy by enriching it in the nobler component. This is a potentially complex process, but if it is assumed that the noble metal ion has a low concentration and therefore deposits under limiting current conditions, i_{lim} , in the off-times, then $i_{\text{corr}} = i_{\text{lim}}$. Under these conditions, the alloy composition (in terms of the mole fraction of the nobler component, X_N) can be related to the pulse parameters by the expression:

$$X_N = i_{\text{corr}} / \varepsilon_N i_p \theta \quad [3]$$

where ε_N is the current efficiency for deposition of the noble metal, and the other terms have been defined previously.^{22,23} This equation illustrates how the alloy composition depends on the dimensionless parameters θ and i_{corr}/i_p (see Fig. 3). Note that Eq. 3 is only valid in the situation where the corrosion current is non-zero.^{22,23} The full assumptions underlying this equation and the corresponding equation for the no-corrosion case are discussed in a later section.

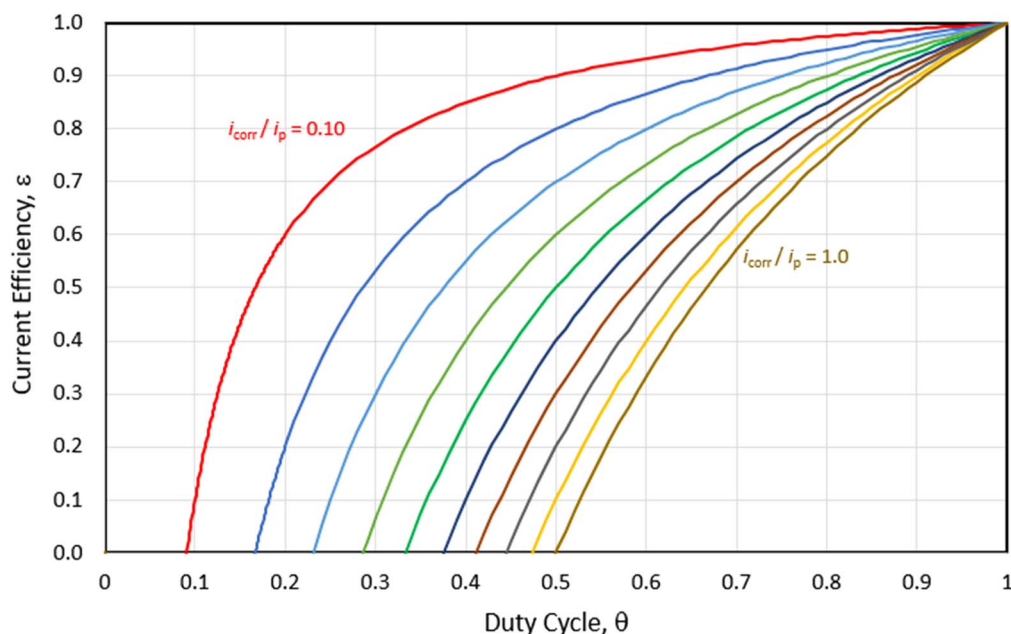


Figure 2. Dependence of the overall current efficiency, ε , as a function of the duty cycle, θ , and the ratio of the corrosion current density, i_{corr} , to the peak current density, i_p , as predicted by Eq. 2 and assuming $\varepsilon' = 1$. Range of i_{corr}/i_p values are 0.1 to 1.0 in steps of 0.1.

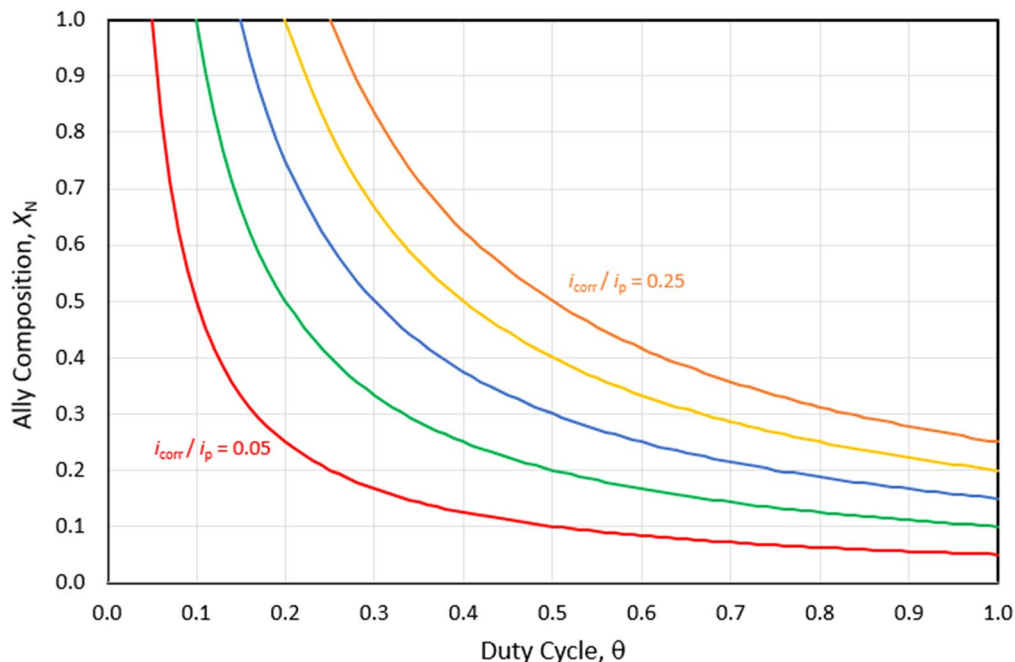
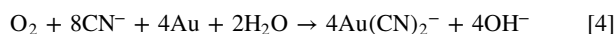


Figure 3. Dependence of the alloy composition (mole fraction of noble component, X_N), as a function of the duty cycle, θ , and the ratio of the corrosion current density, i_{corr} , to the peak current density, i_p , as predicted by Eq. 3 and assuming $\varepsilon_N = 1$. Range of i_{corr}/i_p values are from 0.05 to 0.25 in steps of 0.05.

These simple equations will be employed later to analyse a number of pulse plating systems, but the assumption of a constant i_{corr} in the off-time is not always applicable and various transport, kinetic and passivation phenomena may intervene to ensure this is not the case. For example, the corrosion of copper in chloride containing solutions has been shown to vary through the off-time,^{18,20} and for displacement reactions the corrosion rate tends to slow through the off-time due to increased surface coverage of the more noble component.^{22–24} Additionally, it is possible to find examples of alloy systems where displacement and normal corrosion reactions occur simultaneously.¹⁹ Such systems require a more sophisticated analysis than the one presented here. Nevertheless, these simple models clearly indicate the influence of pulse parameters on the current efficiency and alloy composition given a known (or estimated) corrosion rate.

Analysis of Corrosion Types

Oxygen induced corrosion.—The first example demonstrating the importance of corrosion reaction in pulse plating was a study by Cheh,⁶ who compared the maximum deposition rates possible under pulse and DC plating conditions. For this study, phosphate, citrate and cyanide gold plating solutions were used, but in all cases the depositing species was the $\text{Au}(\text{CN})_2^-$ complex. Under most pulse conditions explored, there was a good agreement between the experimental limiting current density and rate of deposition, and theoretical predictions. However, for the cyanide system there were significant deviations at low duty cycles, and this was attributed to the following corrosion reaction occurring in the off-time:

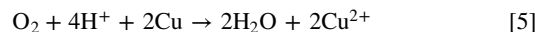


The rate of this corrosion reaction was determined independently under equivalent hydrodynamic conditions and found to be $i_{\text{corr}} = 0.82 \text{ mA cm}^{-2}$. Using this value, the author was able to achieve much better agreement between the theoretical predictions and experimental data. The fact that corrosion was not seen in citrate and phosphate solutions reflects that there were no free cyanide ions to aid the dissolution, or alternatively, that the gold is passive in these electrolytes. Applying Eq. 2 to Cheh's data ($i_p = 18.9 \text{ mA cm}^{-2}$, $i_{\text{corr}} = 0.82 \text{ mA cm}^{-2}$ and assuming that $\varepsilon' = 1$)

the following current efficiencies can be extracted; $\varepsilon = 0.83$ ($\theta = 0.20$), $\varepsilon = 0.94$ ($\theta = 0.40$) and $\varepsilon = 0.97$ ($\theta = 0.60$). Therefore, even when i_{corr} is only 5% of i_p , the current efficiency can be significantly impacted at low duty cycles.

A second example was provided by West and co-workers¹⁹ in 2012, who investigated the pulse plating of copper-silver alloys from an acid copper plating bath for interconnect applications. The amount of silver incorporated is less than 1 wt% so that the deposit approximates pure copper, but the system is relatively complex as three corrosion processes can occur in the off-time: normal O_2 corrosion, comproportionation and displacement. The author's main objective was to predict the Ag-Pd alloy composition during pulse plating when all three types of corrosion were occurring simultaneously. In this section, only the first of these corrosion types will be discussed.

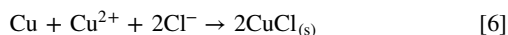
In acidic solutions the overall reaction for oxygen induced corrosion can be written as:



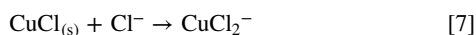
This typically occurs under mass transport control, and at an RDE rotating $\omega = 400 \text{ rpm}$, the corrosion rate was estimated to be 2.7 nm min^{-1} ($i_{\text{corr}} = 0.12 \text{ mA cm}^{-2}$). This is in relatively good agreement with a previous report⁴⁶ of oxygen-induced copper seed layer etching (5 nm min^{-1}) in an acid copper plating bath, albeit under different hydrodynamic conditions. This is around 1% of the value of i_p (10 mA cm^{-2}) but at the low duty cycles used ($\theta = 0.10$), Eq. 2 predicts that $\varepsilon = 0.89$ representing a significant impact on the current efficiency. The peak current and duty cycle were, however, unusually low in this study. Typically, acid copper pulse plating processes tend to operate at higher peak currents and duty cycles where the corrosion effect would be much smaller.^{47–49} This explains why the current efficiency in copper pulse plating tends to be close to unity, even in the presence of dissolved oxygen.

Corrosion via comproportionation reactions.—The first reported example of a corrosion reaction involving comproportionation, was a copper pulse plating study performed by Hibbert in the 1980s.¹⁸ In this investigation, galvanostatic pulse plating was performed from an acidic chloride solution. During the on-time,

copper was deposited in a two-step process, but in the off-time a comproportionation reaction between the deposited Cu and solution Cu^{2+} occurs leading to the formation of insoluble CuCl :



High-purity copper with minimally included CuCl could only be obtained with short off-times, but it was the author's intent to produce pure CuCl deposits so it could be used as a battery anode material. These could be formed optimally at longer off-times, but at some point, the amount of CuCl produced declined due to the formation of soluble Cu(I) halides:



This is perhaps an unusual corrosion reaction, initially leading to the formation of an insoluble salt film which can then be solubilised, but is nevertheless an instructive early example. For reaction 6 the authors measured an initial corrosion rate of $i_{\text{corr}} = 2.1 \text{ mA cm}^{-2}$, but this declined with the off-time.

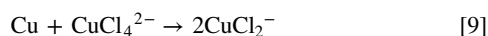
A more recent example relates to the previously discussed study by West¹⁹ on the pulse plating of copper from a chloride-free acid copper solution. These authors noted the importance of O_2 corrosion, but also considered corrosion due to the comproportionation reaction occurring in the off-time according to:



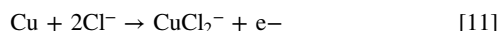
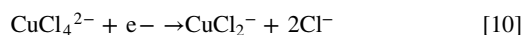
Based on thermodynamic and transport considerations, a corrosion rate of 2.9 nm min^{-1} ($i_{\text{corr}} = 0.13 \text{ mA cm}^{-2}$) was estimated. This was comparable to the corrosion rate due to dissolved O_2 , and the overall corrosion rate in the off-time is likely to represent equal contributions from both processes.

A final corrosion example involving comproportionation was observed during the pulse plating of copper from a chloride-containing deep eutectic solvent (DES) at an RDE.^{20,21} Although copper could be deposited under nearly all conditions, in many instances only partial plating was observed and current efficiencies were low. This effect was greatest at low duty cycles and/or when the off-time was long, and at duty cycles of $\theta = 0.10$ net deposition was not observed. This phenomenon was attributed to a corrosion reaction occurring in the off-time, and this was also supported by the observation that in the off-time the measured potential, E , adopted a mixed potential which did not reflect the reversible or open circuit potential (OCP) of copper.^{20,21}

In the DES system, copper is deposited in a two-step process involving cupric and cuprous chloro-complexes in the on-time, while in the off-time corrosion occurs by the following comproportionation reaction:



The likelihood of this reaction was deduced from the steady-state polarisation, which showed that this could arise from the following coupled cathodic and anodic half-reactions:^{21,50}

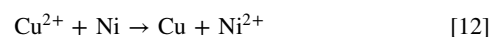


The inherent non-uniform current distribution prevailing at the RDE in the on-time resulted in a large centre to edge thickness variation, and this was removed uniformly in the off-time by corrosion (Fig. 4). For long off-times, corrosion often caused complete removal of the deposit at the centre leaving an annulus of plated copper.^{20,21}

The rate of this corrosion reaction was determined in separate experiments under steady-state conditions as $i_{\text{corr}} = 3.45 \text{ mA cm}^{-2}$. However, substitution of this value into Eq. 2 predicted lower current efficiencies than were observed experimentally, even though

it explained the main trends in the data. A variety of other models were then explored, the most plausible one indicating that the corrosion rate in the off-time is being controlled by a slow chemical dissolution step. This explained the main observations and predicts that, only for long pulse periods will the steady-state corrosion rate be attained.²⁰ Note that oxygen corrosion is also possible in the deep eutectic solvent, but the measured rate under comparable hydrodynamic conditions is very small ($i_{\text{corr}} = 0.025 \text{ mA cm}^{-2}$) and this can be neglected.⁵¹ This low value reflects the low solubility and diffusivity of O_2 in DES systems.

Corrosion via displacement reactions.—Corrosion in pulse plating due to displacement (exchange) reactions is a more common phenomenon, and has been reported^{22–43} in many binary and ternary alloy systems. This has been observed predominantly in aqueous systems,^{22–40} but also in molten salt⁴¹ and ionic liquid^{42,43} systems. As discussed earlier, the main effect is that during the off-time the more noble component deposits and displaces the less noble component. For the deposition of Cu-Ni alloys from citrate electrolytes,^{22–24} the relevant reaction is:



This results in an enrichment of the alloy content of the nobler component (Cu), relative to the situation where displacement does not occur. The main requirement for displacement is that there is a thermodynamic driving force—i.e. one based upon the differences in the standard or reversal potentials of the two alloy components. As with other corrosion reactions, they can be understood in terms of mixed potential theory, and the overall rate of displacement may be strongly influenced by mass transport, kinetics, or surface passivation.^{52,53}

The occurrence of a displacement reaction in the Cu-Ni citrate system can be rationalised by considering the partial and total current for copper and nickel as a function of potential (Fig. 5).^{22–24} This indicates that the nobler component (Cu) deposits under limiting current conditions, while the less noble one (Ni) deposits or dissolves under kinetic control. In the on-time, deposition of Ni and Cu both occur, the former under kinetic control and the latter under mass transport control. In the off-time, under open circuit conditions, a mixed potential of E_{corr} develops where Cu deposits at the limiting current and Ni dissolves. Note that not all displacement systems correspond to this situation, but these characteristics make it easier to develop a simple model.

The earliest studies of this phenomenon by Roy and Landolt focussed on the Cu-Ni ^{22–24} and Cu-Co ^{25,26} systems and this is where the important mechanistic and phenomenological aspects were identified. The electrodeposition of such binary alloys is typically performed from solutions containing a low concentration of the nobler component and a higher concentration of the less noble component. As noted previously, the nobler component deposits under mass transport control (limiting current conditions) while the less noble under kinetic control. In the off-time the nobler component continues to deposit (by displacement) under limiting current conditions, leading to a corresponding amount of dissolution of the less noble component and this suggests that it deposits at a constant rate throughout the entire pulse period.

This situation was modelled numerically for the Cu-Ni system²² and the results indicated that the surface concentration of Cu^{2+} ions was zero throughout the entire pulse period and that the partial current for copper, i_{Cu} , corresponds to the steady-state limiting current, $i_{\text{lim,Cu}}$. Under these conditions, a simple expression can be used to predict the copper content in the alloy:

$$X_{\text{Cu}} = \frac{i_{\text{lim,Cu}}}{\theta i_p} \quad [13]$$

where X_{Cu} is the mole fraction of copper, $i_{\text{lim,Cu}}$ is the limiting current for copper deposition, and the other parameters have been

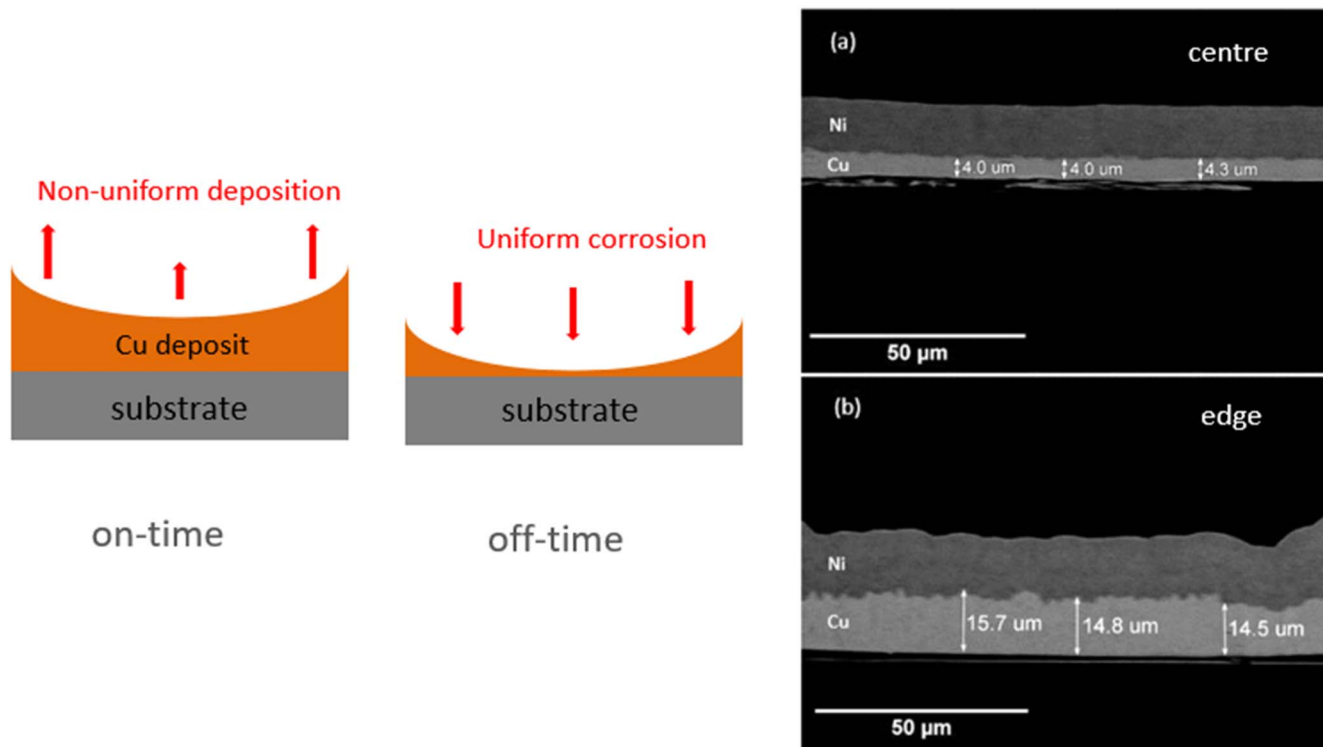


Figure 4. Schematic showing non-uniform deposition in the on-time, and uniform corrosion in the off-time for the Cu-DES system.²⁰ The resulting Cu deposit revealed in SEM cross-sections is thicker at edges relative to the centre. Note that post Cu deposition, a Ni layer has been over-plated to allow sectioning.

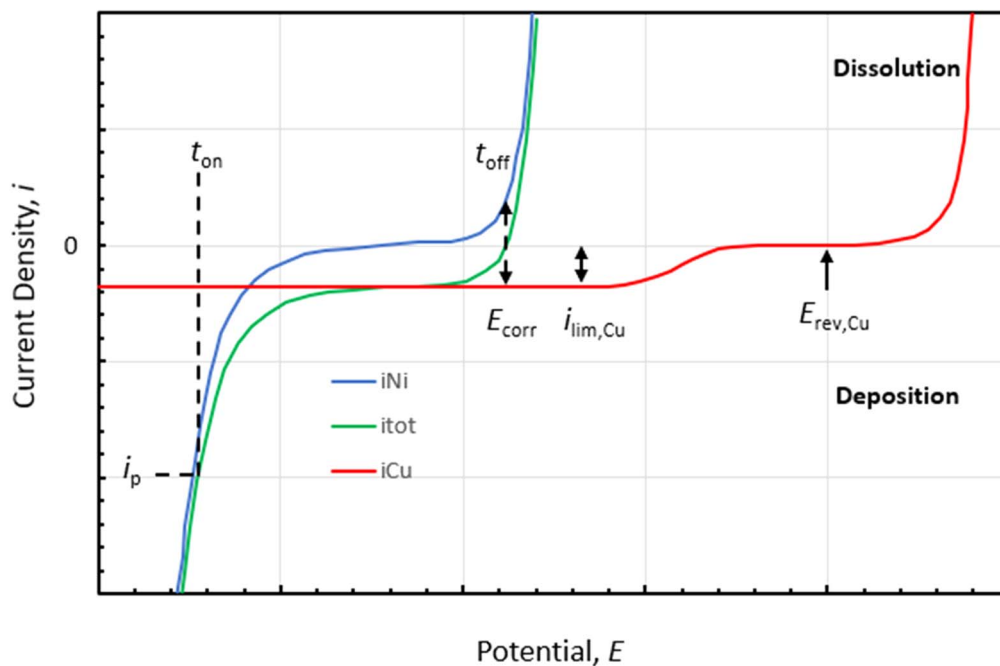


Figure 5. Partial current densities for the deposition and dissolution of nickel (i_{Ni}) and copper (i_{Cu}) as a function of applied potential, E . The total current is the sum of the two partial currents ($i_{tot} = i_{Ni} + i_{Cu}$). Copper deposits under mass transport conditions at a rate of $i_{lim,Cu}$. In the on-time, plating is performed at a peak current of i_p , and in the off-time the corrosion (mixed) potential corresponding $i_{tot} = 0$ is given by E_{corr} . The corrosion rate is $i_{corr} = i_{lim,Cu}$.

defined previously. This is referred to as the corrosion model (CM) and Eq. 13 indicates that the alloy composition is dependent on the duty cycle but is independent of the pulse period. This expression is identical to Eq. 3 with $i_{lim,Cu} = i_{corr}$ and assuming that $\epsilon_N = \epsilon_{Cu} = 1$.

The alternate no-corrosion model (NCM) assumes that displacement reactions do not occur in the off-time, so deposition only

occurs in the on-time and the copper concentration gradient relaxes in the off-time. The alloy composition predicted by the no-corrosion model requires a modified expression which allows for the fact that copper deposition occurs under transient conditions in the on-time and that there is no copper deposition (or nickel dissolution) in the off-time:

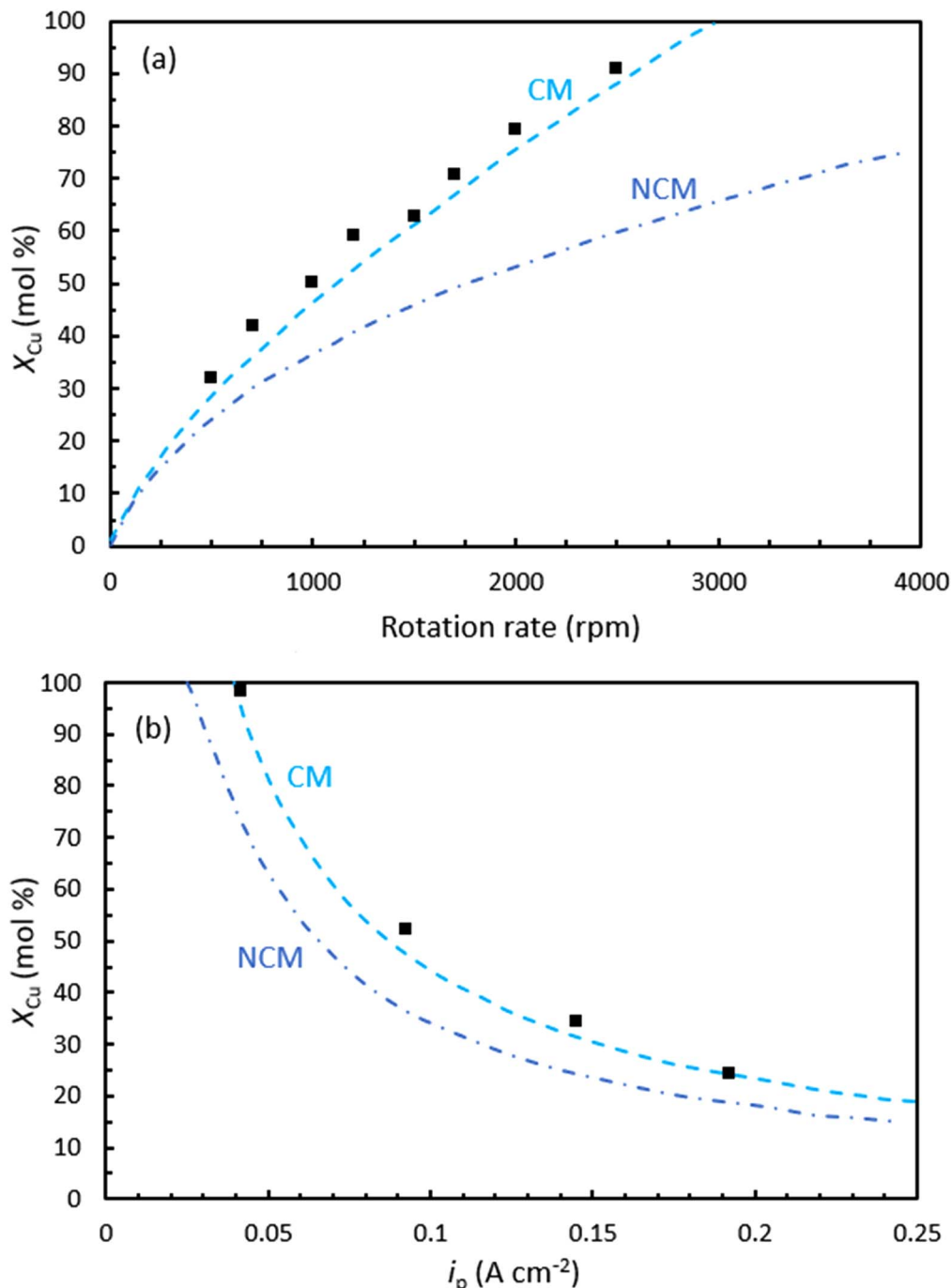


Figure 6. Testing the validity of the CM and NCM models for the pulse plating of Cu-Ni alloys at a rotating cylinder electrode (RCE) by comparing measured and predicted alloy composition as a function of (a) the hydrodynamic conditions at the RCE, (b) the peak current, i_p . The CM line is calculated from Eq. 13 and NCM line from Eq. 14. Adapted from Ref. 22.

$$X_{Cu} = \frac{\int_0^{ton} i_{Cu} dt}{i_p T \theta} \quad [14]$$

$$X_{Cu} = \frac{i_{lim,Cu}}{i_p} \quad [15]$$

where i_{Cu} is the partial current for copper deposition in the on-time. This expression shows that the alloy composition depends on both the pulse period and the duty cycle. For the NCM case, and for relatively long pulse periods where steady-state conditions are being approached, the copper content in the alloy can be approximated to:

These models have been applied to Cu-Ni alloys pulse plated from a citrate electrolyte and the results obtained were in good agreement with the corrosion model.^{22,23} Figure 6, for example, shows that the copper content in the alloy as function of pulse and hydrodynamic conditions is consistent with the corrosion (CM) model. The corrosion model was also validated for the pulse plating of Ni-Cu

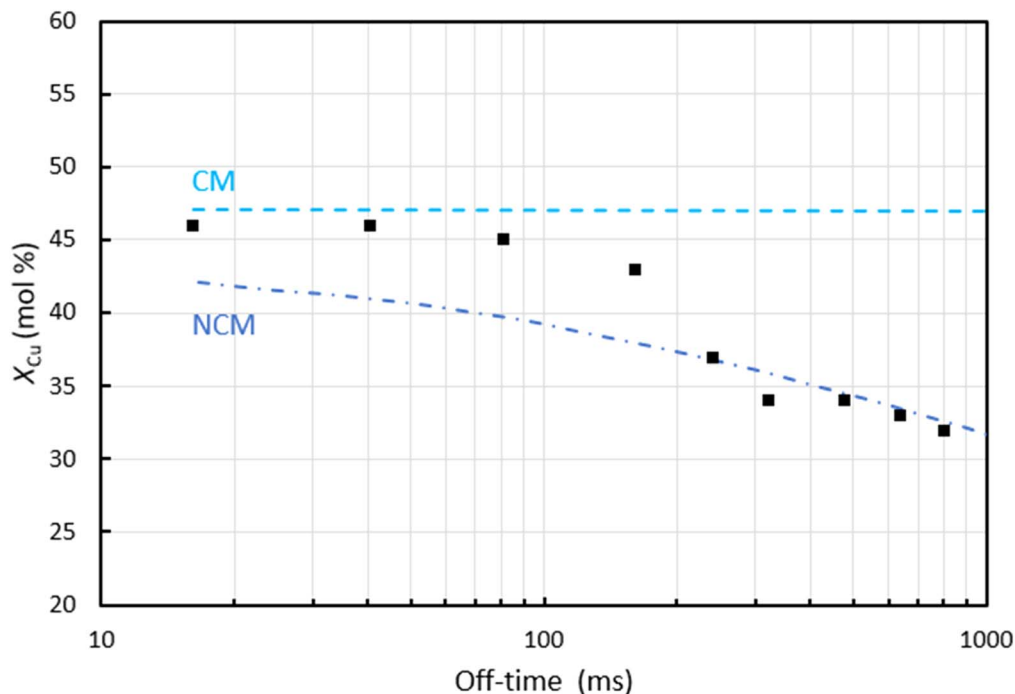


Figure 7. Effect of the off-time on the copper content in the Ni-Cu alloy, indicating the transition from the corrosion model (CM) to the no-corrosion model (NCM) at long times. The duty cycle is fixed at $\theta = 0.20$, $i_p = 50 \text{ mA cm}^{-2}$ and $i_{\text{corr}} = i_{\text{lim}} = 5.6 \text{ mA cm}^{-2}$. The CM line is calculated from Eq. 13 and NCM line from Eq. 14. Adapted from Ref. 23.

alloys from sulfamate electrolytes,²⁴ Cu-Co and Co-Fe-Cu alloys from citrate electrolytes,^{25,26} Cu-Al from a chloroaluminate molten salt,⁴¹ and therefore has a wide applicability.

The corrosion model generally fits the data best at shorter times when the amount of the noble component deposited by displacement does not significantly cover the surface. However, at long off-times the surface will become increasingly blocked, and the rate of displacement will decline.^{23–25} At sufficiently long off-times, when a continuous layer of the nobler component has formed, the displacement reaction will cease. For this reason, the corrosion model typically applies at relatively short off-times, and for longer off-times the alloy composition will tend to correspond to the no-corrosion model.^{22–25} At intermediate off-times, the predicted alloy composition is expected to transition from the CM to the NCM case. This behaviour has been verified in a number of systems (Fig. 7). Compared to the limiting cases, this intermediate time region is more complex to model, although some attempts have been made in this regard.⁵⁴ A simpler approach is to assume that the corrosion model applies until a critical time corresponding to the formation of an inhibiting copper layer, and beyond this time the no-corrosion model applies.^{23,25}

Following these initial studies of the pulse plating of Cu-Co and Cu-Ni alloys, displacement effects were noted in a wide range of other binary alloy systems including: Ag-Pd,¹⁹ Sn-Bi,^{28,29} Pt-Ru,³⁰ Mn-Cu,³¹ Zn-Mn,^{32,33} Au-Cu,³⁴ Fe-Ni,³⁷ Re-Ni,³⁸ Cu-Sn³⁹ and Cd-Te.⁴⁰ It was also shown to occur during the pulse plating of ternary alloys such as Co-Fe-Co,²⁶ Au-Ni-C⁵⁵ and Pb-Sn-Cu.³⁶ All of these studies are from aqueous electrolytes, but there have also been reports of displacement effects altering alloy composition during the pulse deposition of In-Sn and Co-Al from room temperature ionic liquids^{42,43} and Cu-Al from molten salts.⁴¹ Table I summarizes some of the important characteristics of these experiments.

Most investigations have focused entirely on the effect of displacement on alloy composition, but a few studies have looked at its influence on deposit microstructure.^{29,32,34} For example, in a study of Sn-Bi alloys the displacement reaction was demonstrated to have a strong influence on microstructure, and promoted an equiaxed

rather than a columnar grain structure.²⁹ In an investigation of the pulse plating of Au-Cu alloys, it was noted that the grain size typically increased with off-time. It was suggested that the displacement reaction initiates a rearrangement of atoms in the alloy, which promotes grain growth.³⁴ However, such recrystallisation is normally expected in the off-time during pulse plating, unless adsorbed species act to stabilise small grains.^{4,13} A final example is a pulse plating study of Zn-Mn alloys from a citrate-EDTA electrolyte.³² During the off-time, displacement occurred predominantly with the γ -Mn phase leading to its complete dissolution, and this resulted in a monophasic deposit containing only ϵ -ZnMn.

Unambiguous proof of displacement effects would normally require demonstration of enrichment with the noble element with off-time (or duty cycle), measurement of a mixed potential in the off-time, and ideally an in situ determination of the corrosion/displacement rate with an electrochemical quartz crystal microbalance (EQCM). Some authors^{30,38,55} have also employed ex situ surface analysis techniques (e.g. AES or XPS) to establish if displacement had occurred. In a study of the Au-Cu system,³⁴ the XRD pattern of the deposit was determined as a function of the off-time. This indicated (Fig. 8) a shift in the position of the major (111) peak which indicated a decrease in the composition of copper (i.e. the less noble component) and is consistent with a displacement process.

Table II summarises some of the more important characteristics of the various types of corrosion processes encountered in pulse plating studies.^{6,19–21,56} In most cases, the corrosion rate has been determined in separate dissolution experiments, but in the case of the Cu-Co displacement reactions it is via an in situ measurement with a rotating EQCM.⁵⁶ Typically, the corrosion rate is controlled by mass transport of the oxidant species, but for the Cu-DES and Cu-Co sulfamate systems, $i_{\text{corr}} < i_{\text{lim}}$ suggesting that they are under mixed control.

Other susceptible system.—Although reports of corrosion in pulse plating studies are relatively limited in number, it is likely they occur to some degree in other systems. An obvious candidate is the silver-cyanide system which is often employed in pulse and pulse-

Table I. Summary of major studies involving displacement effects in the pulse plating of alloys. Note that in many cases the displacement reactions have been simplified and assume that the metal ions are not complexed.

Alloy System	Plating Solution	Noble Component	Displacement Reaction	Evidence for Displacement	Notes
Cu-Ni ²²⁻²⁴	aqueous citrate ^{22,23} or sulfamate ²⁴	Cu	$\text{Cu}^{2+} + \text{Ni} \rightarrow \text{Cu} + \text{Ni}^{2+}$	mixed potential, off-time	Uses CM/NCM model
Cu-Co ²⁵	aqueous sulfamate	Cu	$\text{Cu}^{2+} + \text{Co} \rightarrow \text{Cu} + \text{Co}^{2+}$	mixed potential, off-time	Also, EQCM data in Ref. 56
Ag-Cu ¹⁹	aqueous sulfate	Ag	$2\text{Ag}^+ + \text{Cu} \rightarrow 2\text{Ag} + \text{Cu}^{2+}$	effect of off-time	
Sn-Bi ^{28,29}	aqueous citrate ²⁸ or MSA ²⁹	Bi	$2\text{Bi}^{3+} + 3\text{Sn} \rightarrow 2\text{Bi} + 3\text{Sn}^{2+}$	mixed potential, off-time	Uses CM/NCM model Anomalous alloy content
Cu-Al ⁴¹	molten salt - chloroaluminate	Cu	$3\text{Cu}^+ + \text{Al} \rightarrow 3\text{Cu} + \text{Al}^{3+}$	mixed potential, off-time	
Co-Al ⁴³	ionic liquid - PBC	Co	$3\text{Co}^{2+} + 2\text{Al} \rightarrow 3\text{Co} + 2\text{Al}^{3+}$	other (see note)	
In-Sn ⁴²	ionic liquid—EMI-BF ₄ -Cl	Sn	$3\text{Sn}^{2+} + 2\text{In} \rightarrow 3\text{Sn} + 2\text{In}^{3+}$	off-time	
Zn-Mn ^{32,33}	aqueous citrate ³² or chloride ³³	Zn	$\text{Zn}^{2+} + \text{Mn} \rightarrow \text{Zn} + \text{Mn}^{2+}$	off-time	
Cu-Mn ³¹	aqueous sulfate	Cu	$\text{Cu}^{2+} + \text{Mn} \rightarrow \text{Cu} + \text{Mn}^{2+}$	unspecified	XPS, also EQCM data in Ref. 64
Pt-Ru ^{30,64}	aqueous chloride	Pt	$3\text{Pt}^{2+} + 2\text{Ru} \rightarrow 3\text{Pt} + 2\text{Ru}^{3+}$	off-time	
Cu-Sn ³⁷	aqueous pyrophosphate	Cu	$\text{Cu}^{2+} + \text{Sn} \rightarrow \text{Cu} + \text{Sn}^{2+}$	inferred	Inferred from XPS
Mn-Co ²⁷	aqueous sulfate	Co	$\text{Co}^{2+} + \text{Mn} \rightarrow \text{Co} + \text{Mn}^{2+}$	mixed potential, off-time	
Re-Ni ³⁸	aqueous citrate	Re	$\text{ReO}_4^- + 2\text{H}^+ + \text{Ni} \rightarrow \text{ReO}_3^- + \text{Ni}^{2+} + \text{H}_2\text{O}$	other (see note)	
Au-Cu ³⁴	aqueous sulfite/EDTA	Au	$2\text{Au}^+ + \text{Cu} \rightarrow 2\text{Au} + \text{Cu}^{2+}$	off-time	Also inferred by XRD
Fe-Ni ³⁷	aqueous sulfate/chloride	Ni	$\text{Ni}^{2+} + \text{Fe} \rightarrow \text{Ni} + \text{Fe}^{2+}$	off-time	
Cd-Te ⁴⁰	aqueous acid sulfate	Te	$\text{HTeO}_2^+ + 3\text{H}^+ + 2\text{Cd} \rightarrow \text{Te} + 2\text{Cd}^{2+} + 2\text{H}_2\text{O}$	other (see note)	Inferred from modelling
Co-Fe-Cu ²⁶	aqueous acetate	Cu	$\text{Cu}^{2+} + \text{Co(Fe)} \rightarrow \text{Cu} + \text{Co}^{2+} (\text{Fe}^{2+})$	off-time	Ternary system, uses CM/NCM
Au-Ni-C ³⁵	aqueous citrate	Au	$2\text{Au}^+ + \text{Ni} \rightarrow 2\text{Au} + \text{Ni}^{2+}$	off-time	Ternary system
Pb-Sn-Cu ³⁶	aqueous fluoborate	Cu	$\text{Cu}^{2+} + \text{Pb} \rightarrow \text{Cu} + \text{Pb}^{2+}$	off-time	Ternary system

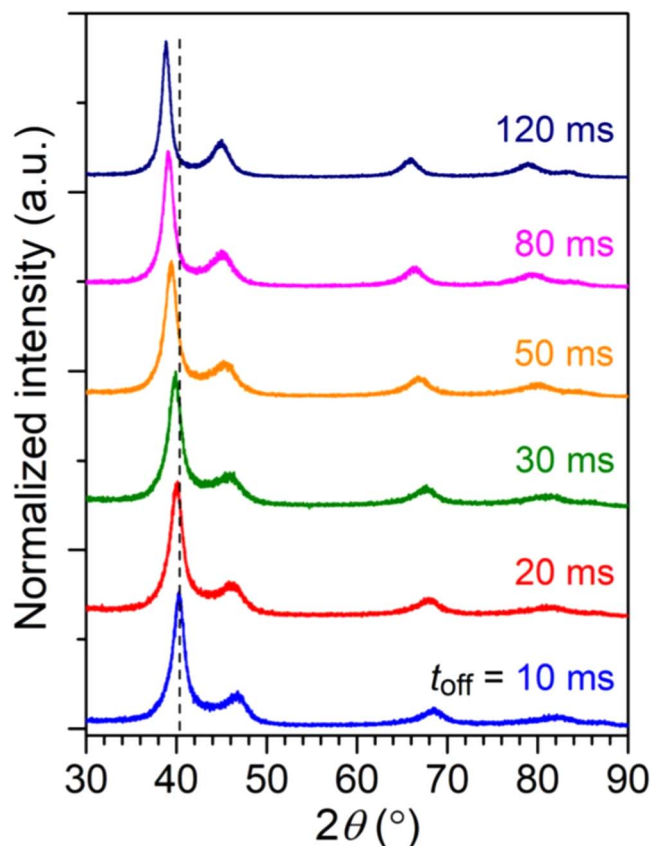


Figure 8. Variation in the XRD pattern of an Au-Co alloy deposited by pulse plating ($i_p = 20 \text{ mA cm}^{-2}$ and $t_{\text{on}} = 10 \text{ ms}$) as the off-time is varied. The shift in the (111) peak from $2\theta = 40.2^\circ$ to 38.8° with t_{off} is consistent with a decrease in Cu content of the alloy. From. Ref. 34.

reverse plating.^{1,2} Silver is also prone to dissolution in oxygenated cyanide-based electrolytes, and the available data indicates that the rate is typically 50%–100% higher than for gold under equivalent conditions (e.g. pH, cyanide and O_2 concentrations).⁵⁷ It is probable that corrosion is important in this system, but the available publications lack sufficient detail to evaluate its extent. In particular, there is an absence of data showing the current efficiency as a function of duty cycle or off-time, or any potential monitoring that might indicate the formation of a mixed potential in the off-time.

It should be noted that the corrosion effects due to comproportionation are quite general and are possible in redox systems where there is a stable, intermediate valency species.⁵⁰ This could occur in aqueous, RTIL or molten salt systems. Typical examples would be the pulse deposition of Fe(III) and Cr(III) species from chloride-containing deep eutectic solvents^{58,59} or equivalent aqueous system. Other representative examples would be the deposition of V(III) species from LiCl-KCl molten salts⁶⁰ or Nb(V) deposition from

molten fluoride salts.⁶¹ All of these systems have been investigated under DC conditions, but their electrochemical characteristics indicate that they would be susceptible to corrosion by comproportionation if pulse plating was implemented. In some cases, it may be feasible to reduce the electroactive species to a lower oxidation state (e.g. Cu(I), Fe(II), Cr(II) or Nb(IV)) where comproportionation cannot occur.

The occurrence of corrosion in pulse-plated binary and ternary alloys via displacement is also expected to be more widespread than the available literature suggests. In many cases, corrosion is likely to have occurred, but has not been considered by the authors. Invariably, one alloy component will be nobler than the other, and under these conditions a displacement process is inevitable. Other factors (e.g. passivation, kinetics or mass transport) may intervene to minimise these effects, but a thermodynamic driving force for displacement reactions is usually present. Even in the Sn-Pb alloy system, where there is a small difference ($<0.02 \text{ V}$) in reversible potentials of the components in acid solutions, additives are employed which shift the potentials further apart. This is to allow better control of alloy composition and to improve deposit properties, but also makes them more susceptible to displacement effects.⁶²

Monitoring corrosion effects.—A number of approaches have been developed to monitor the presence of corrosion reactions during pulse plating. In the case of the corrosion of metals via oxygen corrosion or comproportionation reactions, perhaps the simplest method is to monitor the current efficiency as a function of the duty cycle or the off-time. The most preferred approach is to keep t_{on} and i_p constant and vary the off-time as this ensures that the current efficiency is not being influenced by other considerations (e.g. mass transport or kinetics). For example, Fig. 9 illustrates how the current efficiency for Cu(II) deposition from a DES system decreases as a function of increasing off-time due to corrosion via a comproportionation reaction.^{20,63} In contrast, in the case of the Sn(II)-DES system where comproportionation is not possible, the current efficiency is constant with off-time.⁶³

A similar method can be used to evaluate the importance of corrosion reactions in the pulse deposition of binary and ternary alloys. As shown in previous sections, there is a tendency for the concentration of the noble element in the alloy to increase in the presence of a displacement reaction. The enrichment of the noble component due to displacement will increase with the off-time, and this is often fairly unambiguous evidence of a displacement process. Of course, the corrosion rate declines with time, and its self-limiting nature will manifest itself at long off-times resulting in a constant alloy composition. Figure 10, for example, shows this phenomenon for two representative systems^{32,41} and this approach has been used by other workers^{23,24,29,34–36,41} to establish the importance of a displacement mechanism.

Another useful means of assessing corrosion is to monitor the electrode potential during current pulsing. In the absence of corrosion effects, the measured potential, E , during the off-time should revert back to the reversible or open circuit potential as determined by steady-state polarisation data. However, in the presence of a corrosion reaction, the potential in the off-time will

Table II. Summary of pulse plating studies where corrosion effects have been quantified, and their major characteristics.

System	Type of Corrosion	Rate (mA cm^{-2})	Rate Control	Corrosion Reaction
Au citrate/cyanide ⁶	oxygen	0.82	mass transport	$4\text{Au} + \text{O}_2 + 8\text{CN}^- + 2\text{H}_2\text{O} \rightarrow 4\text{Au}(\text{CN})_2^- + 4\text{OH}^-$
Cu acid sulphate ¹⁹	oxygen	0.12	mass transport	$2\text{Cu} + \text{O}_2 + 4\text{H}^+ \rightarrow 2\text{Cu}^{2+} + 2\text{H}_2\text{O}$
Cu acid sulfate ¹⁹	comprop	0.13	mass transport	$\text{Cu} + \text{Cu}^{2+} \rightarrow 2\text{Cu}^+$
Cu acid chloride ¹⁸	comprop	2.1	—	$\text{Cu} + \text{Cu}^{2+} + 2\text{Cl}^- \rightarrow 2\text{CuCl}_{(\text{s})}$
Cu DES (ethaline) ²⁰	comprop	3.45	mixed	$\text{Cu} + \text{CuCl}_4^{2-} \rightarrow 2\text{CuCl}_2^-$
Cu-Co sulfamate ⁵⁶	displace	0.5–2.5	mixed	$\text{Cu}^{2+} + \text{Co} \rightarrow \text{Cu} + \text{Co}^{2+}$
Cu acid chloride ⁶⁸	comprop	2.3	—	$\text{Cu} + \text{CuCl}_{2(\text{aq})} + 4\text{Cl}^- \rightarrow 2\text{CuCl}_3^{2-}$
Zn acid sulfate ⁶⁷	acid	0.60	kinetic	$\text{Zn} + 2\text{H}^+ \rightarrow \text{Zn}^{2+} + \text{H}_2$

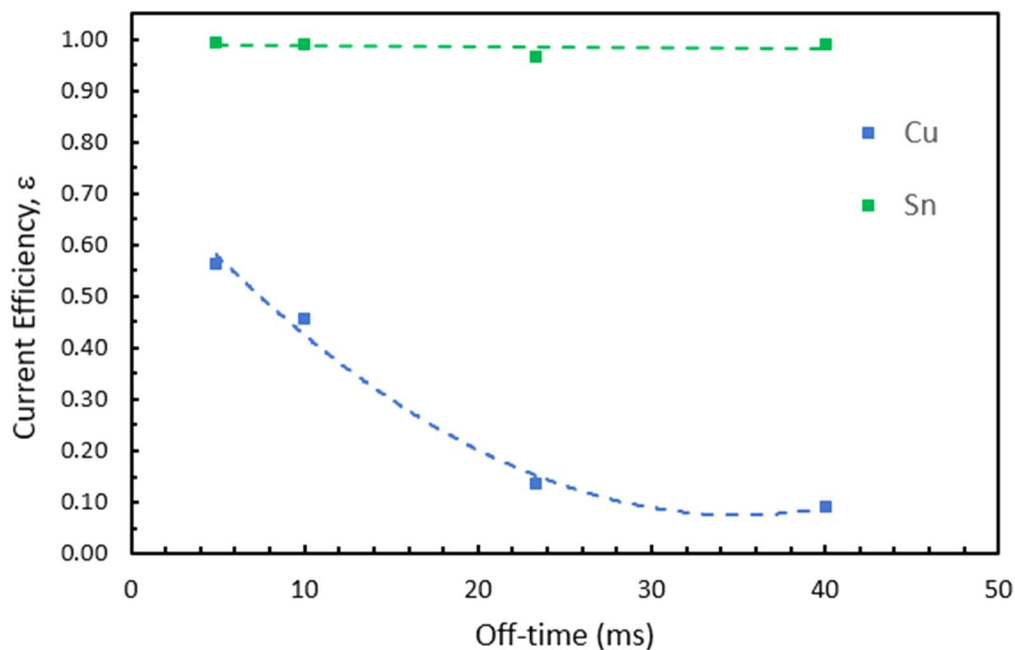


Figure 9. Effect of the off-time on the current efficiency, ϵ , for copper and tin deposition from a deep eutectic solvent.^{20,63} This illustrates that corrosion is occurring only in the copper system. Note that pulse and DC limiting current are not exceeded in either system, and in both case i_p and t_{on} are fixed, so any changes in current efficiency must reflect a corrosion process.

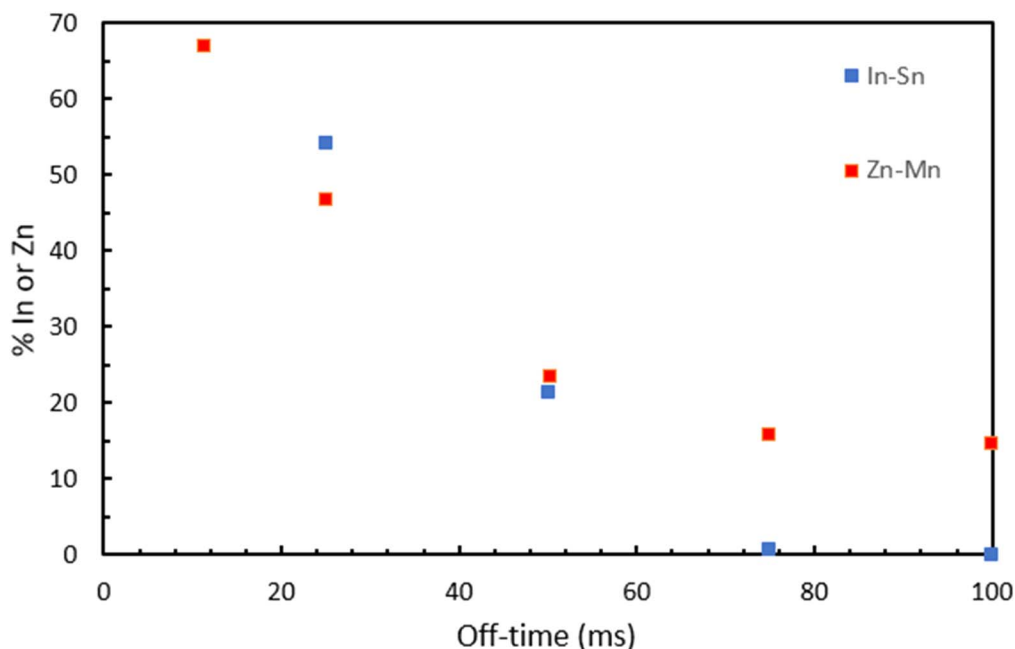


Figure 10. Variation in the alloy composition with off-time for two different alloy systems demonstrating the occurrence of a displacement reaction. The first data set is the pulse plating of In-Sn from a RTIL⁴² ($i_p = 30 \text{ mA cm}^{-2}$ and $t_{on} = 1 \text{ ms}$); the second is Zn-Mn deposition from an aqueous electrolyte³² ($i_p = 40 \text{ mA cm}^{-2}$ and $t_{on} = 50 \text{ ms}$).

adopt a mixed potential that is characteristic of the corroding system. Such behaviours are shown in Fig. 11 for the Sn(II)-DES system and the Cu(II)-DES systems.^{20,63} The approach can also be used to demonstrate the occurrence of displacement in the electrodeposition of alloys.²² In this case, a mixed potential will also develop characteristic of the displacement reaction, which is not related to the OCP of the system determined separately in polarisation measurements. In the limit of full surface coverage, the potential will shift to the reversible potential of the noble metal. This approach

has been used in a number of studies^{25,27,28,42} and again illustrates the usefulness of measuring E as a diagnostic in pulse plating.

The most effective means for determining if corrosion is occurring is to measure the mass change in the off-time in situ using an EQCM. Assuming that the measured frequency change in the off-time is related purely to change in the mass of the deposit, this would show unambiguously corrosion was occurring. Such an approach has been employed in the case of the pulse deposition of Cu-Co⁵⁶ and Pt-Ru⁶⁴ alloys (Fig. 12). In both cases, the mass change in the off-time was

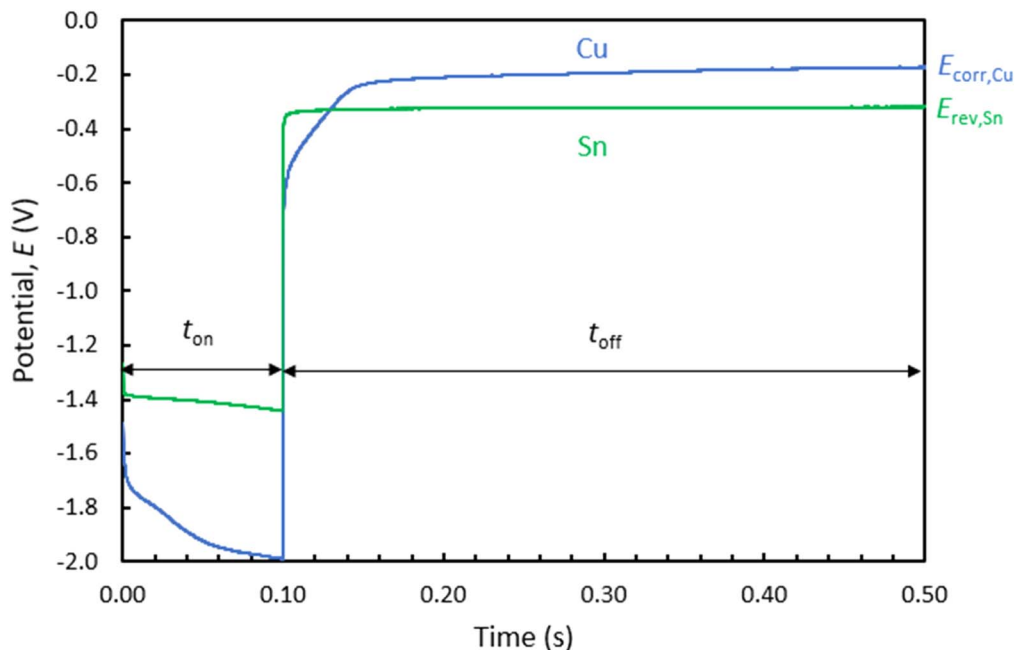


Figure 11. Variation of the electrode potential, E , in the on-time and off-time periods for copper and tin deposition from a deep eutectic solvent.^{20,63} For tin, the potential returns to the reverse potential, E_{rev} , in the off-time. For copper, the potential in the off-time corresponds to a mixed potential, $E_{\text{corr}} \approx -0.20$ V, rather than the reversible potential ($E_{\text{rev}} \approx +0.60$ V).

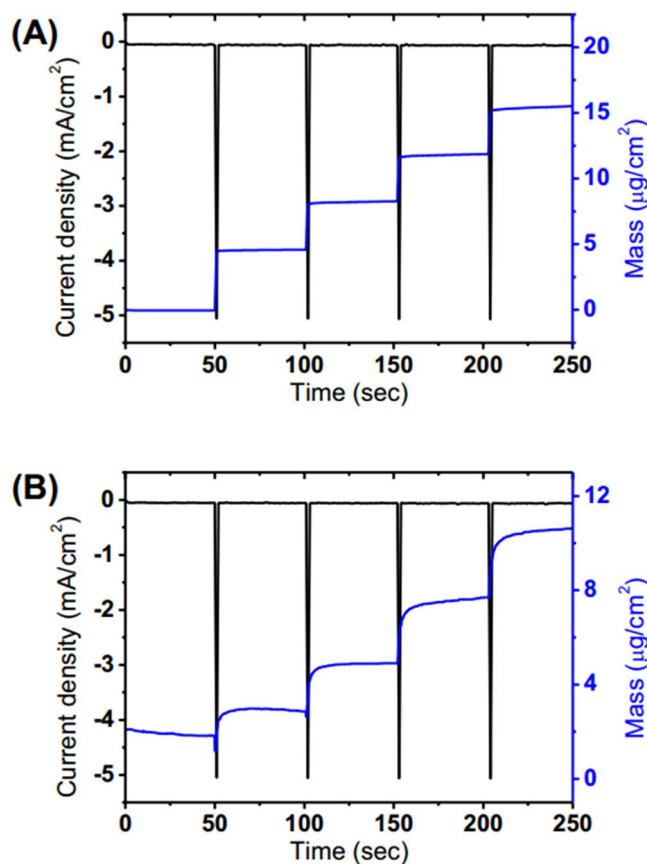


Figure 12. Mass change determined by EQCM for pulse current deposition in an electrolyte containing: (A) 10 mM Pt^{2+} (B) 5 mM Pt^{2+} + 5 mM Ru^{3+} . For (B) there is a mass increase in the off-time due to the deposition of Pt and dissolution of Ru according to the displacement reaction: $3\text{Pt}^{2+} + 2\text{Ru} \rightarrow 3\text{Pt} + 2\text{Ru}^{3+}$. From Ref. 64.

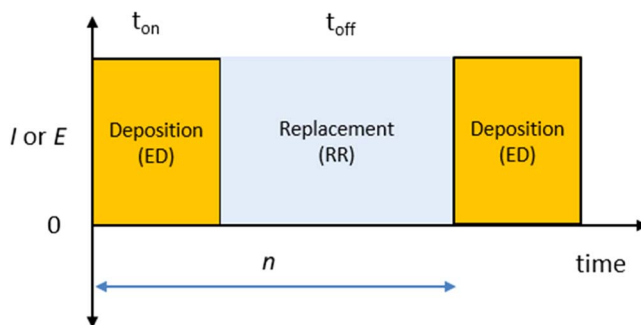


Figure 13. A schematic diagram of the electrodeposition-redox replacement (EDRR) process along with key parameters.⁶⁶ Deposition of the less noble materials occurs in the on-time and can be performed under constant current, I , or potential, E , conditions. In the off-time, deposition of the noble component occurs by a replacement (displacement) reaction. The process is repeated for n cycles.

consistent with a displacement reaction occurring, and for the Cu-Co study the overall corrosion rate was assessed.⁵⁶ This was of the order of $i_{\text{corr}} = 2.5 \text{ mA cm}^{-2}$ for a pulse period of $T < 0.1$ s, but declined to 0.5 mA cm^{-2} for pulse periods of $T = 10\text{--}100$ s due to increased coverage of Cu. Notably in this study, i_{corr} was always below the limiting current ($i_{\text{lim}} = 4.0 \text{ mA cm}^{-2}$) for Cu deposition.

There are some practical difficulties with time resolution when short pulse periods are used, and a lack of sensitivity when the alloy components have similar atomic masses, but the EQCM technique appears to be the most direct approach to identifying and quantifying corrosion effects. Interestingly, the authors of the Cu-Co study subsequently used this approach to demonstrate the absence of corrosion in the Ni-Mo alloy system.⁵⁵ The reasons for the lack of corrosion were not addressed, but may relate to surface passivation or the blocking action of adsorbed reaction intermediates.

Minimising corrosion effects.—In the case of oxygen corrosion, a number of choices can be made to minimise corrosion effects. An

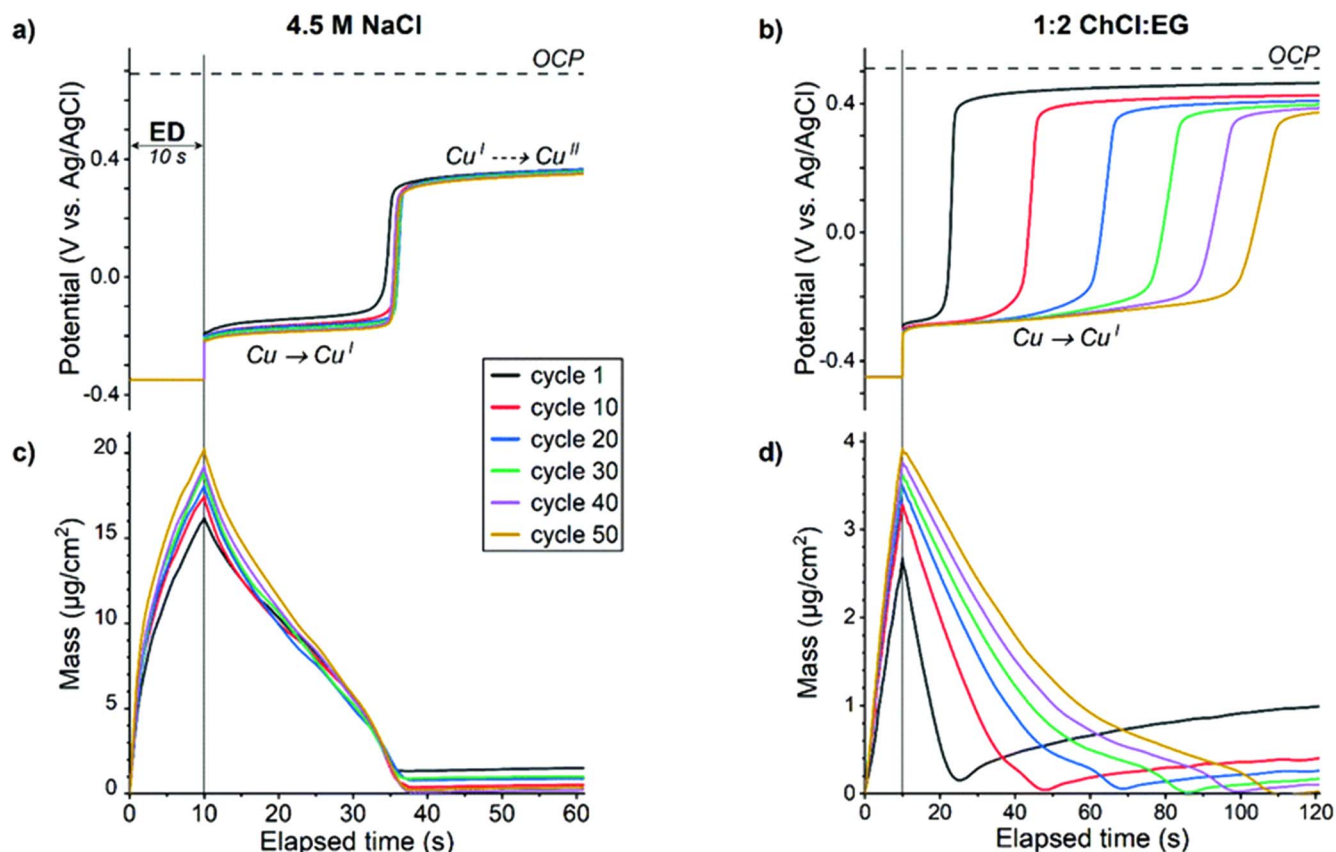


Figure 14. EQCM and potential data for the EDRR process performed in aqueous chloride (a) and (c) system and a deep eutectic solvent (b) and (d). The vertical grey lines delineate the on-time ($t < 10$ s) and the off-time ($t > 10$ s). For (c) corrosion dominates for $10 \text{ s} < t < 35 \text{ s}$ and displacement for $t > 35 \text{ s}$. Reproduced from⁶⁸ with permission from the Royal Society of Chemistry under Creative Commons Attribution 3.0 Unported Licence.

obvious approach is to remove O_2 from the solution, but this is not often practical in an industrial plating situation. Oxygen-induced corrosion is typically mass-transport controlled and reduced agitation is likely to decrease the rate, but this also reduces the maximum plating rate. For both comproportionation and oxygen corrosion, some common methods of reducing their effects are available. Firstly, it could be reduced by operating at longer duty cycles (i.e. $\theta > 0.50$), however, this limits the available parameter space where the process can be optimised and, in effect, DC conditions are being approached. It may also be possible to maintain the current or potential in the off-time to a value that prevents dissolution, but allows for minimal deposition. Importantly, most pulse rectifiers are not able to deliver exactly zero current in the off-time, and a small anodic or cathodic offset current is usually present. This additional complication has been noted by some workers.^{22,24,27}

Another approach is to employ corrosion inhibitors, and these may also function as additives that modify the deposit characteristics. In the case of the pulse deposition of copper from a deep eutectic solvent (1:2 ChCl:EG) it was demonstrated that the use of a benzotriazole (BTA) additive resulted in improved current efficiencies but it also promoted surface roughness.²⁰ Collectively this was achieved by improving the current efficiency in the on-time, and by reducing the rate of corrosion in the off-time. However, the use of BTA compounds poses various environmental issues associated with their toxicity and their difficulty in removal using water treatment plants,⁶⁵ and more environmentally friendly corrosion inhibitors need to be investigated.

For alloy deposition, a number of similar approaches are available. For example, it was shown for the deposition of Cu-Co alloys, the use of saccharin inhibited the displacement reactions.⁵⁶ Likewise, avoiding short duty cycle (or long off-times) will minimise these effects, but this also restricts the range of alloy

compositions that might be attained. If the less noble component can undergo passivation during the off-time, this will also inhibit the corrosion reaction. The use of passivating electrolytes may facilitate this, but often experiments are performed in chloride-containing electrolytes or molten salts where passivation is unlikely. Interestingly, in the Cu-Ni sulfamate system steady-state polarisation data suggested that nickel would be passive in the potential range explored, but under pulse plating (transient) conditions passivation was not observed and the displacement reaction proceeded normally.²⁴ Studies of the cementation of Cu on Ni in sulfuric acid have also shown that copper deposition occurs even when the mixed potential is in a region where nickel is normally passive.⁵²

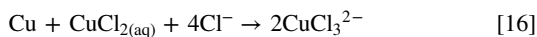
Another suggested approach to minimise the influence of the displacement reaction on alloy composition is to impose a cathodic current in the off-time at a value corresponding the limiting current for the reduction of the noble metal.⁴¹ This would still allow for its deposition in the off-time but there is no corresponding dissolution of the less noble component by displacement. The end result is that the enrichment of the more noble metal is reduced compared to the case where displacement is occurring. This approach was demonstrated for the pulse plating of Cu-Al alloys from a molten salt but the overall effect on composition was relatively small.⁴¹

Corrosion effects in the electrodeposition - redox replacement (EDRR) processes.—A useful variant of pulse plating where displacement and corrosion effects are both important is the electrodeposition-redox replacement (EDRR) process which has been developed for trace metal ion recovery.^{66–68} In the EDRR process, a less noble component (e.g. Cu, Zn or Ni) is deposited on an electrode in the on-time, while in the off-time a noble metal (e.g. Ag, Pt or Au) is deposited by a displacement (replacement) reaction. The off-time is selected to be of sufficient length to ensure that

essentially all the less noble metal is displaced, and the processes is repeated through many cycles (Fig. 13). This ensures that the resulting deposit contains predominantly the noble component, and this method has been shown to be competitive with other hydro-metallurgical processes for extracting high-value metals from waste streams.⁶⁶

One potential complication with the EDRR process is corrosion of the less noble metal in the off-time, and this has been noted in a number of studies.^{66–68} This is undesirable as it results in a loss of the less noble component and this reduces the amount of the nobler material that can be deposited by displacement in the off-time. For example, during the recovery of Ag by displacement on to a Zn layer from acidic solutions, corrosion of Zn in the off-time by H⁺ ions was demonstrated to occur.^{66,67} The process was monitored using an EQCM and clearly shows a mass accumulation in the on-time (Zn deposition) followed by a mass loss at the beginning of the off-time (Zn corrosion), and finally at longer times a mass increase as the displacement process dominated. The average corrosion rate at the beginning of the off-time (i.e. before displacement starts) estimated from the EQCM data is $i_{\text{corr}} = 0.60 \text{ mA cm}^{-2}$.

The influence of corrosion and displacement effects was studied in greater detail in a subsequent paper where Au was recovered on to Cu layers from an aqueous chloride (4.5 M NaCl) or a deep eutectic solvent (1:2 ChCl:EG).⁶⁸ The process was also monitored with an EQCM and revealed evidence of a corrosion process occurring at the beginning of the off-time (Fig. 14). In the aqueous chloride system, this was attributed to the following comproportionation reaction:



The average copper corrosion rate measured in the EDRR experiment under essentially stagnant conditions was $i_{\text{corr}} = 2.28 \text{ mA cm}^{-2}$. A similar corrosion process was observed in the deep eutectic solvent and this was also attributed to a comproportionation reaction (i.e. Eq. 9). Collectively, the EDRR results indicate the importance of corrosion effects in the off-time, regardless of the manner in which pulse plating is implemented. Table II compares the corrosion characteristics encountered in normal pulse plating and in the EDRR variant. Also note the similarity to the earlier example of the pulse plating of Ag-Cu alloys where both corrosion and displacement were observed in the off-time.¹⁹

Conclusions

The importance of corrosion effects in the off-time period when metals and alloys are pulse plated has been reviewed. The available literature indicates that, for pure metals, two main forms can be identified—conventional oxygen-induced corrosion, and corrosion by comproportionation reactions. The main effect of these corrosion reactions is to reduce the deposition rate and the overall current efficiency. The number of reported instances of these types of corrosion is relatively small, but other susceptible systems have been identified. A simple equation relating the current efficiency to the corrosion rate and pulse parameters is described, and this can be used to estimate its overall importance. Some recommendations are also made in regard to monitoring corrosion processes and selecting appropriate conditions to minimise such effects.

For the pulse plating of alloys, the main corrosion processes encountered in the off-time are due to displacement reactions. These modify the alloy composition, by enriching it with the nobler component, and can also influence the deposit microstructure. This phenomenon has been observed for the deposition of binary and ternary alloys, and has been reported in both aqueous and non-aqueous electrolytes. A simple model has been developed to quantify such effects and the applicability and limitations of such an approach have been discussed. While such effects are almost inevitable in the pulse plating of alloys, some suggestions on how to check for the occurrence of displacement processes and minimise their effect on alloy composition are made.

Practitioners of pulse plating and the related EDRR process are advised to always consider the possibility of corrosion in the off-time—whether it be by comproportionation, oxygen, hydrogen ions, or displacement. In many instances the effects are fairly minor, and even in cases where they are significant, modification of the solution chemistry or pulse parameters can often be used as effective mitigations. In limited cases it may be beneficial, for example, allowing the attainment of alloy compositions that would not normally be realisable, or by making favourable modifications to the deposit microstructure. Although the EDRR process exploits displacement to recover noble metals, other types of corrosion in the off-time are undesirable and can represent a significant loss in both process and energy efficiency.

As discussed earlier, the simplest method for verifying the importance of corrosion in pulse plating is to monitor the potential in the off-time to see if a mixed potential exists. Unfortunately, the majority of pulse plating studies do not undertake such potential monitoring. Corrosion effects can also be initially assessed by examining the changes in the current efficiency or alloy composition as a function of the off-time, and the corrosion rate itself can be determined in situ by the EQCM technique. All of these approaches can be readily implemented in most pulse plating studies and, if undertaken systematically, would allow more corroding systems to be identified and characterised. The authors hope that this review will stimulate more awareness and interest in understanding this neglected phenomenon.

ORCID

T. A. Green  <https://orcid.org/0000-0002-3538-5217>

References

1. J.-C. Puipe and F. Leaman, *Theory and Practice of Pulse Plating*, (AESF, Orlando, Florida) (1986).
2. W. E. G. Hansal and S. Roy, *Pulse Plating* (Eugen Leuze, Bad Saulgau) (2012).
3. E. J. Taylor, *J. Applied Surf. Finish.*, **3**, 178 (2008).
4. N. Ibl, *Surf. Technol.*, **10**, 81 (1980).
5. E. J. Taylor, M. E. Inman, H. M. Garich, H. A. McCrabb, S. T. Snyder, and T. D. Hall, *Electrochemical Engineering: From Discovery to Product*, R. C. Alkire, P. N. Bartlett, and M. T. Koper, (Wiley-VCH) (2018).
6. H. Y. Cheh, *J. Electrochem. Soc.*, **118**, 551 (1971).
7. H. Y. Cheh, *J. Electrochem. Soc.*, **118**, 1132 (1971).
8. D. T. Chin, *J. Electrochem. Soc.*, **130**, 1657 (1983).
9. N. Ibl, *Metalloberfläche*, **33**, 51 (1979).
10. M. Datta and D. Landolt, *Surf. Technol.*, **25**, 97 (1985).
11. S. Roy, *Trans. IMF*, **86**, 87 (2008).
12. T. A. Green and S. Roy, *Trans. IMF*, **95**, 46 (2017).
13. N. Ibl, J. C. Puipe, and H. Angerer, *Surf. Technol.*, **6**, 287 (1978).
14. R. T. C. Choo, A. Toguri, A. M. El-Sherik, and U. Erb, *J. Appl. Electrochem.*, **25**, 384 (1995).
15. J. C. Puipe and N. Ibl, *J. Appl. Electrochem.*, **10**, 775 (1980).
16. S. Roy and D. Landolt, *J. Appl. Electrochem.*, **27**, 299 (1997).
17. J. C. Puipe, *Trans. IMF*, **96**, 244 (2018).
18. C. W. Yeow and D. B. Hibbert, *J. Electrochem. Soc.*, **130**, 786 (1983).
19. I. Volov, E. Swansom, B. O'Brien, S. W. Novak, R. van den Boom, K. Dunn, and A. C. West, *J. Electrochem. Soc.*, **159**, D677 (2012).
20. T. A. Green, X. Su, and S. Roy, *J. Electrochem. Soc.*, **168**, 062515 (2021).
21. T. A. Green, X. Su, and S. Roy, *ECS Trans.*, **77**, 1247 (2017).
22. S. Roy, M. Matlosz, and D. Landolt, *J. Electrochem. Soc.*, **141**, 1509 (1994).
23. S. Roy and D. Landolt, *J. Electrochem. Soc.*, **142**, 3021 (1995).
24. P. Bradley, S. Roy, and D. Landolt, *J. Chem. Soc. Faraday Trans.*, **92**, 4015 (1996).
25. P. E. Bradley and D. Landolt, *Electrochim. Acta*, **45**, 1077 (1999).
26. P. E. Bradley, B. Janossy, and D. Landolt, *J. Appl. Electrochem.*, **31**, 137 (2001).
27. J. Wu, C. D. Johnson, Y. Jiang, R. S. Gemmen, and X. Liu, *Electrochim. Acta*, **54**, 793 (2008).
28. Y.-D. Tsai and C.-C. Hu, *J. Electrochem. Soc.*, **158**, D482 (2011).
29. E. Sandnes, M. E. Williams, M. D. Vaudin, and G. R. Stafford, *J. Electron. Mater.*, **37**, 490 (2008).
30. Y. C. Hsieh, P. W. Wu, Y. J. Lu, and Y. M. Chang, *J. Electrochem. Soc.*, **156**, B735 (2009).
31. F. Mangolini, L. Magagnin, and P. L. Cavalotti, *J. Electrochem. Soc.*, **153**, C623 (2006).
32. C. Muller, M. Sarret, and T. Andreu, *J. Electrochem. Soc.*, **150**, C772 (2003).
33. F. Claudel, N. Stein, N. Allain, A. Tidu, N. Hajczak, and R. Lallement, *J. Appl. Electrochem.*, **49**, 399 (2019).
34. H. Tang, C. Y. Chen, T. F. M. Chang, T. Nagoshi, D. Yamane, T. Konishi, K. Machida, K. Masu, and M. Sone, *J. Electrochem. Soc.*, **165**, D58 (2018).

35. T. Yokoshima, A. Takanaka, T. Hachisu, A. Sugiyama, Y. Okinaka, and T. Osaka, *J. Electrochem. Soc.*, **160**, D513 (2013).
36. T. Sato, M. Kudo, and T. Tachikawa, *J. Met. Finish. Soc. Jpn.*, **39**, 196 (1988).
37. X. P. Li, H. L. Seet, Z. J. Zhao, and Y. K. Kong, *J. Metastable Nanocryst. Mater.*, **23**, 163 (2005).
38. B. A. Rosen, E. Gileadi, and N. Eliaz, *J. Electroanal. Chem.*, **731**, 93 (2014).
39. S. D. Beattie and J. R. Dahn, *J. Electrochem. Soc.*, **150**, C457 (2003).
40. M. W. Verbrugge and C. W. Tobias, *AIChE J.*, **33**, 628 (1987).
41. Q. Zhu and C. L. Hussey, *J. Electrochem. Soc.*, **148**, C395 (2001).
42. M. Noda, M. Morimitsu, and M. Matsunaga, *ECS Trans.*, **3**, 249 (2007).
43. M. R. Ali, A. Nishikata, and T. Tsuru, *Electrochim. Acta*, **42**, 1819 (1997).
44. S. Roy, *Surf. Coat. Technol.*, **105**, 202 (1998).
45. W. R. A. Meuleman, S. Roy, L. Peter, and I. Varga, *J. Electrochem. Soc.*, **149**, C479 (2002).
46. L. Yang, T. Atanasova, A. Radisic, J. Deconinck, A. C. West, and P. Vereecken, *Electrochim. Acta*, **104**, 242 (2013).
47. O. Chene and D. Landolt, *J. Appl. Electrochem.*, **19**, 188 (1989).
48. Q.-B. Wu, T. A. Green, and S. Roy, *Electrochem. Comm.*, **13**, 1229 (2011).
49. W. C. Tsai, C. C. Wan, and Y. Y. Wang, *J. Electrochem. Soc.*, **150**, C267 (2003).
50. T. A. Green, P. Valverde, and S. Roy, *J. Electrochem. Soc.*, **165**, D313 (2018).
51. M.-L. Doche, A. Mandroyan, M. Mourad-Mahmoud, V. Moutarlier, and J.-Y. Hihn, *Chem. Eng. Process.: Process Intensif.*, **121**, 90 (2017).
52. S. Robertson, M. Jeffrey, H. Zhang, and E. Ho, *Metall. Mater. Trans. B*, **36**, 313 (2005).
53. G. P. Power and I. M. Ritchie, *Electrochim. Acta*, **26**, 1073 (1981).
54. P. E. Bradley and D. Landolt, *Electrochim. Acta*, **42**, 993 (1997).
55. A. Marlot, P. Kern, and D. Landolt, *Electrochim. Acta*, **48**, 29 (2002).
56. J. J. Kelly, P. Kern, and D. Landolt, *J. Electrochem. Soc.*, **147**, 3725 (2000).
57. X. Dai and P. L. Breuer, *Hydrometallurgy*, **133**, 139 (2013).
58. R. Bock and S.-E. Wulf, *Trans. IMF*, **87**, 28 (2009).
59. A. P. Abbott, G. Capper, D. L. Davies, and R. K. Rasheed, *Chem. Eur. J.*, **10**, 3769 (2004).
60. J. Gussone, C. R. Y. Vijay, J. Haubrich, K. Milicevic, and B. Friedrich, *J. Appl. Electrochem.*, **48**, 427 (2018).
61. P. Chamelot, P. Taxil, D. Oquab, J. Serp, and B. Lafage, *J. Electrochem. Soc.*, **147**, 4131 (2000).
62. M. Datta et al., *J. Electrochem. Soc.*, **142**, 3779 (1995).
63. X. Su, *PhD Thesis* (University of Strathclyde) (2019).
64. I. T. Lu, Y. C. Hsieh, P. W. Wu, and J. F. Lee, (2011), *Abstract #2447*, 220th ECS Meeting.
65. Z.-Q. Shi, Y.-S. Liu, Q. Xiong, W.-W. Cai, and G.-G. Ying, *Sci. Total Environ.*, **661**, 407 (2019).
66. L. Cui, K. Yliniemi, J. Vapaavuori, and M. Lundstrom, *Chem. Eng. J.*, **465**, 142737 (2023).
67. Z. Wang, P.-M. Hannula, S. De, B. P. Wilson, J. Vapaavuori, K. Yliniemi, and M. Lundstrom, *ACS Sustain. Chem. Eng.*, **9**, 8186 (2021).
68. I. Korolev, S. Spathariotis, K. Yliniemi, B. P. Wilson, A. P. Abbott, and M. Lundstrom, *Green Chem.*, **22**, 3615 (2020).